APL Quantum

RESEARCH ARTICLE | AUGUST 19 2024

Ultra-low density and high performance InAs quantum dot single photon emitters

C. Shang ; M. De Gregorio ; Q. Buchinger ; M. Meinecke ; P. Gschwandtner ; A. Pfenning ; T. Huber-Loyola ; S. Hoefling ; J. E. Bowers

APL Quantum 1, 036115 (2024)
https://doi.org/10.1063/5.0209866

Ultra-low density and high performance InAs quantum dot single photon emitters

Cite as: APL Quantum 1, 036115 (2024); doi: 10.1063/5.0209866
Submitted: 24 March 2024 Accepted: 31 July 2024
Published Online: 19 August 2024

C. Shang,[1,a] M. De Gregorio,[2] Q. Buchinger,[2] M. Meinecke,[2] P. Gschwandtner,[2] A. Pfenning,[2] T. Huber-Loyola,[2] S. Hoefling,[2] and J. E. Bowers[1]

AFFILIATIONS

[1] Institute for Energy Efficiency, University of California Santa Barbara, Santa Barbara, California 93117, USA
[2] Physikalisches Institut, Lehrstuhl für Technische Physik, Julius-Maximilians-Universität, Am Hubland, 97074 Würzburg, Germany

[a] Author to whom correspondence should be addressed: shang00@ucsb.edu

ABSTRACT

We report the development of high quality InAs quantum dots with an ultra-low density of 2×10^7 cm^{-2} on (001) GaAs substrates. A significant reduction in the emission wavelength inhomogeneity has been observed. A representative dot has been characterized under cryogenic temperatures, demonstrating a close-to-ideal antibunching of both the exciton and biexciton emissions with a fitted $g^{(2)}(0) = 0.008$ and 0.059, respectively.

I. INTRODUCTION

The advancement of photonic based quantum technologies is expected to usher in a transformative change in data processing and communication protocols,[1] where photonic qubits are generated and manipulated on demand in the established quantum networks.[2] For such technologies to realize their full functionalities, high efficiency photon counters, linear and non-linear photonic circuits, and single photon and entangled photon pair sources are necessary.[3] Significant improvements have been demonstrated for photon detection[4] and linear circuits.[5] However, significant progress in the development of scalable photon sources is needed for integrated quantum photonics.

Several physical systems have been investigated for single photon generation, including trapped individual ions,[6] defects in semiconductors,[7] isolated molecules,[8] parametric downconversion of laser pulses in non-linear crystals,[9,10] and semiconductor quantum dots (QDs). Although each system has its own merits and there is no clear winner yet, semiconductor quantum dots (QDs), coined as "artificial atoms," are nearly ideal two-level systems that can be deterministically triggered via optical[11] or electrical pumping[12,13] to produce quality indistinguishable single photons and outperform all other platforms on single photon emission rate.[11,14] The radiative cascade decay from a biexciton state (XX) to the ground state through an exciton (X) intermediate state within a QD can be utilized to generate one pair of polarization entangled photons.[15] Despite the challenges to extract the photon pair efficiently[16] and complications induced by the shape and atomistic anisotropy of QDs,[17] QDs remain a strong contender as the sources for polarization entangled photon pairs in memory-based quantum repeaters[18] and other applications in quantum information processing.[19,20] Epitaxially grown QDs also offer compactness and tunable emission properties that can be optimized for specific applications when embedded in optical cavities or photonic crystal structures.[21,22] Site-controlled nucleation of QDs is also possible for deterministic QD placement,[23] although the performance for the site-controlled QDs falls short compared to those grown on planar substrates.[24] The solid-state structures promise simple integration of individual QDs with existing and future photonic integrated circuits for on-chip single photon and entangled photon pair emitters.

The main hurdle that prevents QDs from serving as a scalable quantum light source is the inhomogeneous broadening, inherent of the statistical nature of the Stranski–Krastanov (S–K) growth mode for QD formation. In this paper, we present the development

of InAs quantum dots with ultra-low density grown by molecular beam epitaxy on a (001) GaAs substrate. The average dot density is 2×10^7 cm^{-2}, which is the lowest demonstrated to date for S–K growth, to the best of our knowledge. This allows for the characterization of each individual dot and enables deterministic integration of these quantum dots into cavities.[25] A significant reduction in the inhomogeneous broadening has been observed as the QDs are "decoupled" during growth at such low densities. A representative InAs QD embedded in a distributed Bragg reflector (DBR) cavity has been characterized at cryogenic temperatures, demonstrating close-to-ideal photon antibunching for both X and XX with short photon lifetimes.

II. EXPERIMENT AND RESULTS

A. Materials growth and characterization

All samples were grown in a Veeco Gen II solid source MBE reactor. To simplify the process of investigating the optimal growth conditions for the ultra-low density QDs, InAs was deposited on (001) GaAs under various growth conditions. The QDs were then capped with GaAs after a growth interruption of 60 s for the QDs to take shape, and the samples were finished with uncapped surface QDs grown under the same conditions as the embedded dots. Regardless of the growth rate and the total amount of InAs deposited, the QDs exhibit the best morphology in terms of the shape and the uniformity at a growth temperature of 490 °C, measured using a pyrometer, and an arsenic overpressure of 1×10^{-6} Torr. Thus, we believe that the absolute arsenic pressure, instead of the commonly believed V/III flux ratio, is the controlling factor for QD morphology. To obtain the lowest QD density at a given deposition rate, the indium flux was terminated immediately upon the observation of 2D–3D transition via reflective high energy electron diffraction (RHEED). The total amount of InAs required for QD nucleation was 2 ML at the given temperature and arsenic overpressure, conveniently independent of the deposition rate. A further reduction in the dot density is achieved by lowering the deposition rate. As shown in Fig. 1(a), the QD density is reduced drastically as the growth rate of InAs is decreased from 0.11 to 0.0055 ML/s, corresponding to the lowest indium flux that could be reliably measured in our MBE reactor. A surface QD density as low as 2×10^7 cm^{-2} is then achieved reproducibly, which is the lowest density reported in the literature to the best of our knowledge. Recent results are briefly summarized in Table I. Such a density enables optical microcavity fabrication with precisely just one QD located inside each cavity on average.[26,32,33]

The photoluminescence of the embedded QDs was examined via hyperspectral imaging at ~4 K. The emission intensity response of each pixel was overlaid with the corresponding spectral response, which allows for the visualization and statistical analysis of the embedded QDs, shown in Figs. 1(b) and 1(c). Figure 1(d) shows the emission wavelengths of more than 50 QDs, illustrating a very narrow inhomogeneous broadening with an emission wavelength range between 918 and 935 nm. We attributed this narrow inhomogeneous broadening to the reduced Oswald ripening effect during the 60 s growth interruption. The material exchange process has potentially been greatly suppressed as the distance between the dots increases with low QD density. This narrow emission wavelength distribution would improve the probability of locating two or more optically QDs. The areal density of the embedded QDs was independently measured to be 2×10^7 cm^{-2} from the hyperspectral images. The DBR cavity was then designed to center at 927 nm. The bottom mirror consists of 22 periods of GaAs/AlAs superlattice, grown at 530 °C, while the top mirror consists of 15 periods, grown at 580 °C. The GaAs cavity thickness is 260.5 nm, schematically shown in Fig. 2(a). Figure 2(b) shows a dip in the reflected

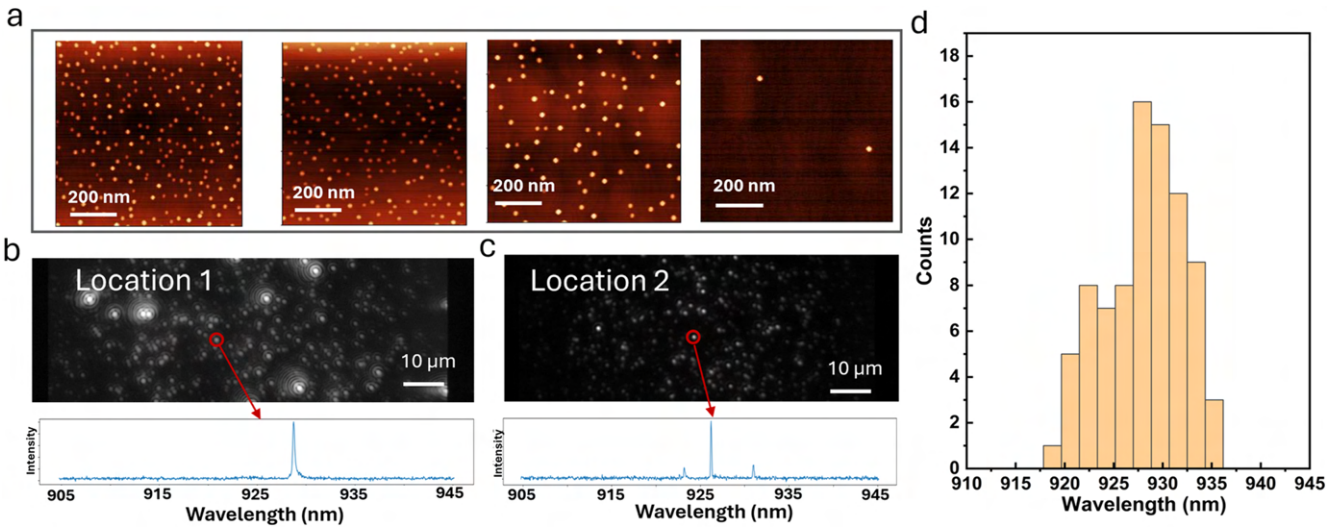

FIG. 1. (a) From left to right, atomic force microscopy images of the surface dots deposited at a rate of 0.11, 0.055, 0.011, and 0.0055 ML/s. The surface dot densities are 4×10^{10}, 2×10^{10}, 4×10^9, and 2×10^7 cm^{-2}, respectively. (b) and (c) Hyper-spectrum imaging of the embedded dots at two different locations, with the emission spectrum of one dot at each location. (d) Emission wavelength distribution of more than 50 dots.

TABLE I. Summary of recent progress on QD density and respective optical performance grown by MBE. DE stands for droplet epitaxy.

Growth method	Density (cm^{-2})	Wavelength (nm)	g2 (0)	QD material	Reference
S–K	10^8	915	0.144	InAs	26
S–K	Mid-10^{10}	1200	0.28	InAs	27
DE	Mid-10^7	780	N/A	GaAs	28
DE	Low-10^7	1470	0.16	GaSb	29
S–K	~10^8	912	0.02	InGaAs	30
S–K	Mid-10^8	1150	N/A	InAs	31
S–K	2×10^7	925	0.008	InAs	This work

signal at 927 nm when shining a white light onto the sample from top down at 4 K, indicating cavity resonance. The spectrum is unnormalized and skewed due to the non-flat intensity distribution for the impinging white light. The QDs are placed at the center of the GaAs cavity. Given a narrow temperature window for high quality QD nucleation (±1.5 °C), the above suggests that the growth temperature has been correctly adjusted accounting for pyrometer reading drift due to the oscillation of surface reflectivity as the DBR growth proceeds.

B. Single photon characterization

To characterize the single photon properties of the InAs QDs, the sample with QDs embedded in a DBR cavity was cooled to 1.6 K. The ultra-low dot density allows for each QD to be characterized individually with a laser spot size of ~1 μm^2. Figure 3(a) shows the emission spectrum of one isolated dot pumped at 880 nm with various pumping powers between 0 and 512 μW. The pumping power is measured before the objective lens and is not corrected for possible transmission loss through the AR coated objective and cryostat windows. The X and the XX emission lines were initially identified by fitting the peak intensities with respect to the pumping power. The X line shown in the inset of Fig. 3(a) illustrates a linear dependence of emission intensity on the pumping power, while the XX line intensity depends on the pumping power in a quadratic manner.[34] To verify the nature of the quasiparticles, cross correlation measurements between the X and the XX lines were conducted. To analyze the single-photon stream by means of time-resolved photon counting, photons from the X and XX lines are first sent to different superconductor nanowire single photon detectors (SNSPDs) after passing through a transmission-grating-monochromator with a holographic grating (1200 grooves/mm). Then, the timestamps for the photon arrival times are correlated as shown in Fig. 3(b), where a clear bunching effect can be observed, suggesting that the X and XX emissions are correlated via the cascading process. The XX emits at a lower energy due to the binding nature of the two electron–hole pairs.[17] The third major peak was then identified as a charged trion from the zero fine structure splitting (FSS), displayed in the polarization series in Fig. 4(a).[35]

To quantify the multiphoton contribution to the individual photon streams from the isolated QD, the emissions for the X and XX line were then each separately sent through a fiber-based 50/50 beam splitter and into different channels onto SNSPDs. The excitation power was 135 μW CW equivalent, with a pulse width of

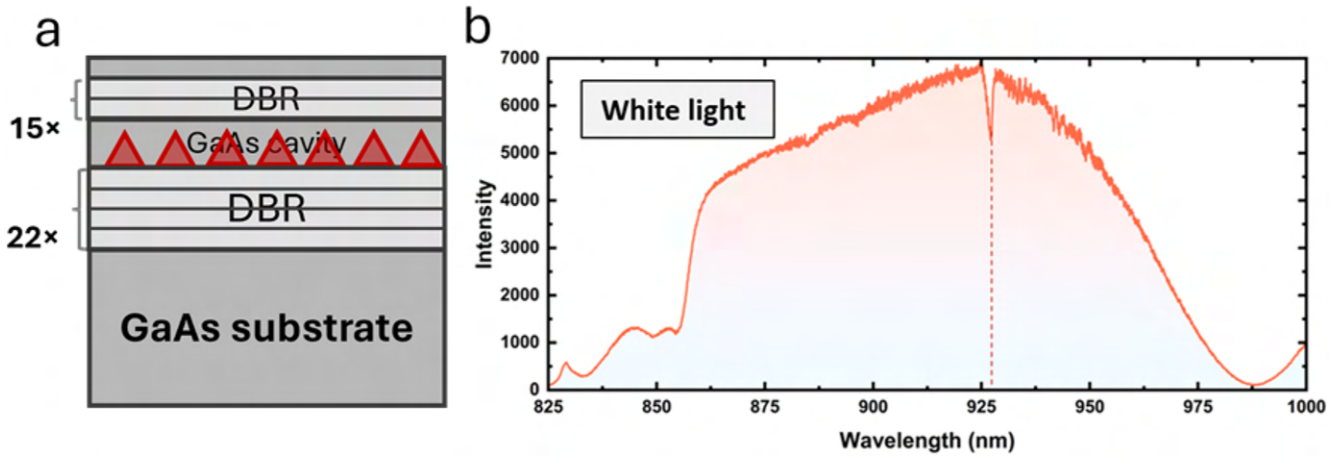

FIG. 2. (a) Schematic of the DBR structure with embedded QDs. (b) The reflected white light signal indicates the cavity resonance to be located at 927 nm as indicated by the dashed line.

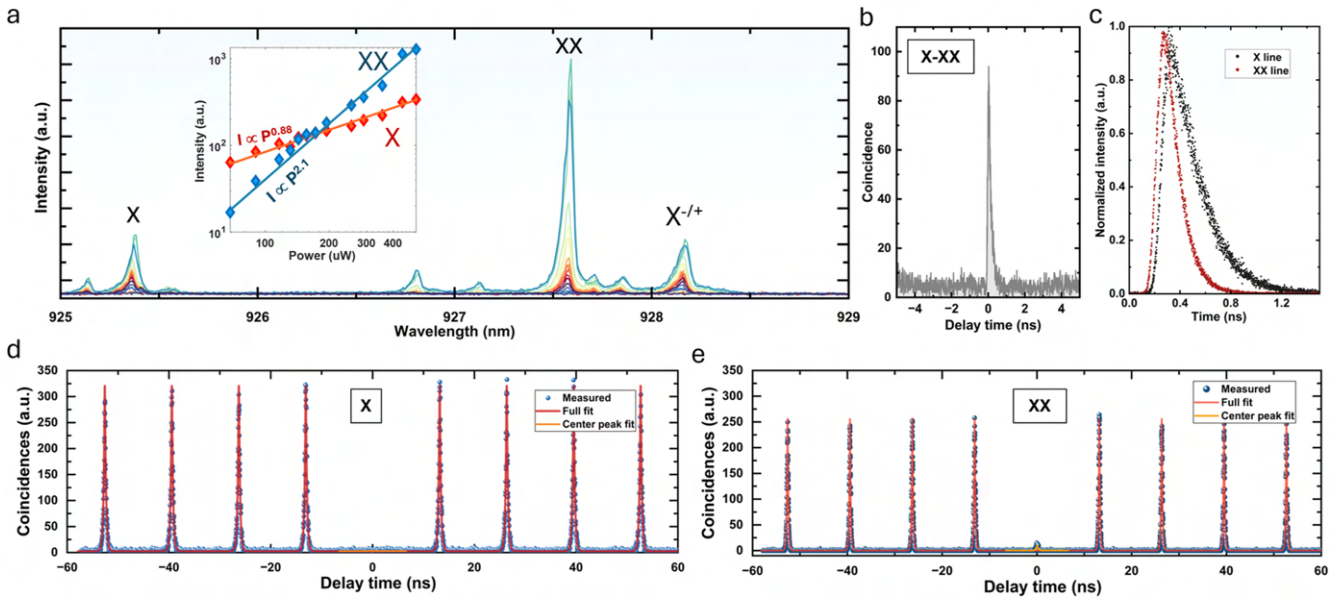

FIG. 3. (a) Power series emission spectra of one representative dot pumped at 880 nm. The inset shows the intensity power dependence of two major peaks X and XX. (b) Cross correlation measurement between X and XX emissions. A clear bunching behavior is observed at zero-time delay. (c) Photon lifetime measurements with pulsed excitation for both the exciton and the biexciton emissions. (d) and (e) Autocorrelation measurement of the X (left) and the XX line (right) under 880 nm pulsed excitation showing antibunching at zero-time delay.

2–3 ps and a period of 13.16 ns. Figures 3(c) and 3(d) demonstrate the resulting coincidence counts in a Hanbury Brown and Twiss setup. The $g^{(2)}(0)$, when normalized, is fitted to be 0.008 for the X emission and 0.059 for the XX emission. The slight rise in the coincidence counts at zero-time delay for the XX line is attributed to the re-excitation of the XX state, which has a significant probability of decay, while the charge carriers are relaxing from their above-band excited state. The multiphoton contribution could be

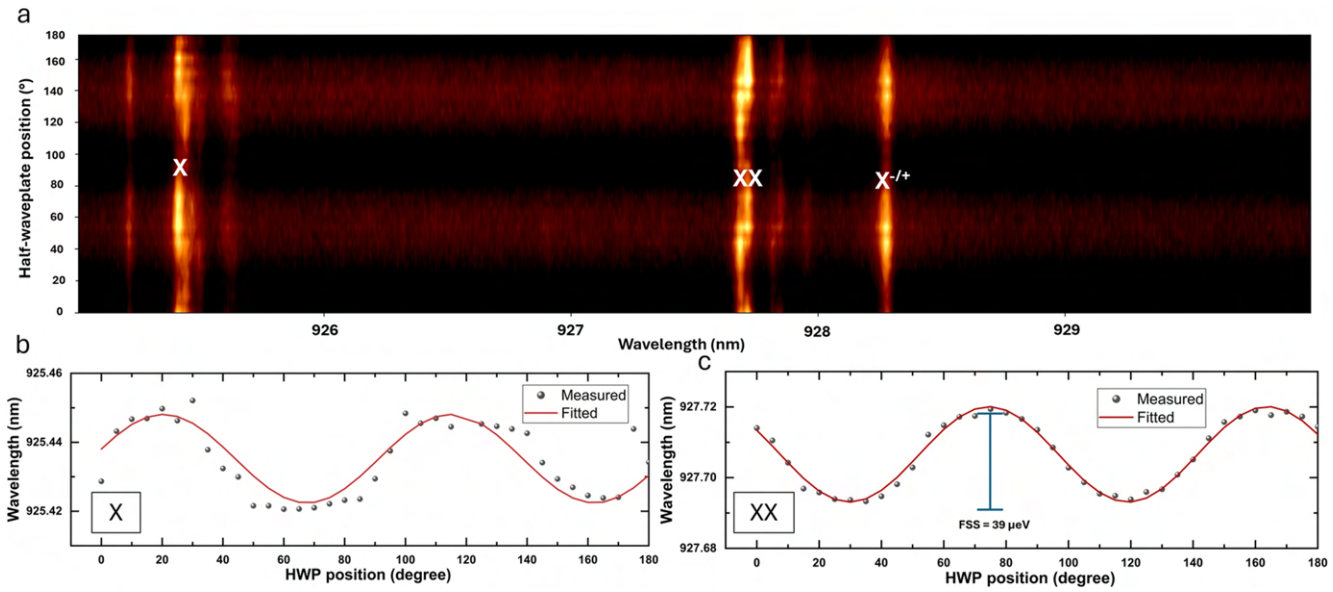

FIG. 4. (a) Emission intensity map with respect to the position of the HWP in a cross-polarization filtering setup. (b) and (c) Extracted peak intensity for X and XX emissions as a function of HWP position, respectively.

even further improved if resonant excitation was implemented for both X and XX photons.[36] The lifetime of the photon emission events determines the upper limit on the operation rate of the source. Figure 3(e) shows the lifetime measurements of the X and XX emissions, where the lifetimes were extracted from mono-exponential fits to be 213 ps for X emission and 113 ps for XX emission. Since the XX state consists of two excitons, where the decay of either exciton is registered as the XX emission, the XX decay rate is anticipated to be roughly twice the decay rate of the X state.[37,38] We expect negligible Purcell enhancement since all measurements were done on dots embedded in a planar DBR cavity where the mode volume extends across the wafer. We then attribute the short lifetimes to possible Ga intermixing. However, we cannot exclude a local perturbation of the cavity that might lead to Purcell enhancement. Such short lifetimes are not only beneficial for higher operation rate and better indistinguishability,[39] but also advantageous in mitigating the influence of the environment and other unwanted processes on the quantum system.[11,40]

FSS of the intermediate X state during cascade emission process from XX to the ground state is another important figure of merit, as the non-zero FSS would reveal the which-path information. This would destroy the polarization entanglement between the photon pairs generated by the cascade process. To characterize the FSS of the above isolated QD, the emission spectra were recorded as we rotated a half-wave plate (HWP) in the common collection and excitation path in 5° increments in combination with a polarizing beam splitter. Since the polarization of the excitation laser is not relevant in above-band excitation, this measurement analyzes the emission only. As shown in Fig. 4(a), a clear oscillation of the emission wavelength has been observed for the X and the XX emissions, but not for the charged X emission.[41] Figures 4(b) and 4(c) show the extracted wavelength of the peak intensity as a function of the HWP angle.[29] The fitted FSS is ~39 μeV, potentially resulting from QD shape anisotropy.[17,42] Such a value is within the commonly reported range[43] and could be further lowered by annealing[44] or added external fields.[45,46]

III. CONCLUSION AND OUTLOOK

In conclusion, we have reproducibly achieved an InAs QD density as low as 2×10^7 cm^{-2} within a resonant cavity by carefully controlling the InAs deposition rate and other related growth conditions, especially the surface temperature uncertainty introduced by the DBR mirrors. A close-to-ideal antibunching effect has been observed for the exciton and biexciton emissions, with a $g^{(2)}(0)$ of 0.008 and 0.059 and a lifetime of 213 and 113 ps, respectively. The sparse placement of the QDs also conveniently facilitated a narrow emission wavelength distribution, which is beneficial for locating two or more optically identical QDs for various quantum applications. This material platform can serve as the building foundation for realizing large scale high quality single photon sources.

ACKNOWLEDGMENTS

This work was funded by the NSF Quantum Foundry at UCSB and German Ministry of Education and Research.

AUTHOR DECLARATIONS

Conflict of Interest

The authors have no conflicts to disclose.

Author Contributions

C.S. and M.D.G. contributed equally to this work.

C. Shang: Conceptualization (lead); Data curation (lead); Formal analysis (lead); Investigation (lead); Writing – original draft (lead); Writing – review & editing (lead). **M. De Gregorio**: Data curation (equal); Formal analysis (equal); Investigation (equal); Writing – review & editing (supporting). **Q. Buchinger**: Data curation (supporting); Writing – review & editing (supporting). **M. Meinecke**: Data curation (supporting). **P. Gschwandtner**: Data curation (supporting). **A. Pfenning**: Data curation (supporting); Investigation (supporting); Supervision (supporting). **T. Huber-Loyola**: Investigation (supporting); Supervision (supporting); Writing – review & editing (supporting). **S. Hoefling**: Funding acquisition (lead); Supervision (lead). **J. E. Bowers**: Funding acquisition (lead); Supervision (lead).

DATA AVAILABILITY

The data that support the findings of this study are available from the corresponding author upon reasonable request.

REFERENCES

[1] J. W. Silverstone, D. Bonneau, J. L. Obrien, and M. G. Thompson, "Silicon quantum photonics," IEEE J. Sel. Top. Quantum Electron. **22**(6), 390–402 (2016).
[2] Y. Arakawa and M. J. Holmes, "Progress in quantum-dot single photon sources for quantum information technologies: A broad spectrum overview," Appl. Phys. Rev. **7**(2), 021309 (2020).
[3] P. Senellart, G. Solomon, and A. White, "High-performance semiconductor quantum-dot single-photon sources," Nat. Nanotechnol. **12**(11), 1026–1039 (2017).
[4] C. M. Natarajan, M. G. Tanner, and R. H. Hadfield, "Superconducting nanowire single-photon detectors: Physics and applications," Supercond. Sci. Technol. **25**(6), 063001 (2012).
[5] J. Carolan *et al.*, "Universal linear optics," Science **349**(6249), 711–716 (2015).
[6] A. Kuhn, M. Hennrich, and G. Rempe, "Deterministic single-photon source for distributed quantum networking," Phys. Rev. Lett. **89**(6), 067901 (2002).
[7] A. Beveratos, R. Brouri, T. Gacoin, A. Villing, J. P. Poizat, and P. Grangier, "Single photon quantum cryptography," Phys. Rev. Lett. **89**(18), 187901 (2002).
[8] B. Lounis and W. E. Moerner, "Single photons on demand from a single molecule at room temperature," Nature **407**(6803), 491–493 (2000).
[9] P. G. Kwiat, K. Mattle, H. Weinfurter, A. Zeilinger, A. V. Sergienko, and Y. Shih, "New high-intensity source of polarization-entangled photon pairs," Phys. Rev. Lett. **75**(24), 4337–4341 (1995).
[10] X. Guo, C. L. Zou, C. Schuck, H. Jung, R. Cheng, and H. X. Tang, "Parametric down-conversion photon-pair source on a nanophotonic chip," Light Sci. Appl. **6**(5), e16249 (2017).
[11] I. Aharonovich, D. Englund, and M. Toth, "Solid-state single-photon emitters," Nat. Photonics **10**(10), 631–641 (2016).
[12] Z. Yuan *et al.*, "Electrically driven single-photon source," Science **295**, 102 (2002).
[13] N. Coste *et al.*, "High-rate entanglement between a semiconductor spin and indistinguishable photons," Nat. Photonics **17**(7), 582–587 (2023).

[14]P. Lodahl, "Quantum-dot based photonic quantum networks," Quantum Sci. Technol. **3**(1), 013001 (2018).
[15]O. Benson, C. Santori, M. Pelton, and Y. Yamamoto, "Regulated and entangled photons from a single quantum dot," Phys. Rev. Lett. **84**(11), 2513–2516 (2000).
[16]Y. Chen, M. Zopf, R. Keil, F. Ding, and O. G. Schmidt, "Highly-efficient extraction of entangled photons from quantum dots using a broadband optical antenna," Nat. Commun. **9**(1), 2994 (2018).
[17]F. Ding *et al.*, "Tuning the exciton binding energies in single self-assembled InGaAs/GaAs quantum dots by piezoelectric-induced biaxial stress," Phys. Rev. Lett. **104**(6), 2–5 (2010).
[18]J. Neuwirth *et al.*, "Quantum dot technology for quantum repeaters: From entangled photon generation toward the integration with quantum memories," Mater. Quantum Technol. **1**(4), 043001 (2021).
[19]H. J. Kimble, "The quantum internet," Nature **453**(7198), 1023–1030 (2008).
[20]N. Gisin and R. Thew, "Quantum communication," Nat. Photonics **1**(3), 165–171 (2007).
[21]J. M. Gérard, B. Sermage, B. Gayral, B. Legrand, E. Costard, and V. Thierry-Mieg, "Enhanced spontaneous emission by quantum boxes in a monolithic optical microcavity," Phys. Rev. Lett. **81**(5), 1110–1113 (1998).
[22]K. Hennessy *et al.*, "Quantum nature of a strongly coupled single quantum dot-cavity system," Nature **445**(7130), 896–899 (2007).
[23]G. Juska, V. Dimastrodonato, L. O. Mereni, A. Gocalinska, and E. Pelucchi, "Towards quantum-dot arrays of entangled photon emitters," Nat. Photonics **7**(7), 527–531 (2013).
[24]J. Große, M. von Helversen, A. Koulas-Simos, M. Hermann, and S. Reitzenstein, "Development of site-controlled quantum dot arrays acting as scalable sources of indistinguishable photons," APL Photonics **5**(9), 096107 (2020).
[25]A. Badolato *et al.*, "Deterministic coupling of single quantum dots to single nanocavity modes," Science **308**(5725), 1158–1161 (2005).
[26]S. Liu *et al.*, "A deterministic quantum dot micropillar single photon source with >65% extraction efficiency based on fluorescence imaging method," Sci. Rep. **7**(1), 13986 (2017).
[27]R. Katsumi *et al.*, "Unidirectional output from a quantum-dot single-photon source hybrid integrated on silicon," Opt. Express **29**(23), 37117 (2021).
[28]P. Atkinson, E. Zallo, and O. G. Schmidt, "Independent wavelength and density control of uniform GaAs/AlGaAs quantum dots grown by infilling self-assembled nanoholes," J. Appl. Phys. **112**(5), 054303 (2012).
[29]J. Michl *et al.*, "Strain-free GaSb quantum dots as single-photon sources in the telecom S-band," Adv. Quantum Technol. **6**(12), 2300180 (2023).
[30]L. Hanschke *et al.*, "Quantum dot single-photon sources with ultra-low multi-photon probability," npj Quantum Inf. **4**(1), 43 (2018).
[31]N. Bart *et al.*, "Wafer-scale epitaxial modulation of quantum dot density," Nat. Commun. **13**(1), 1633 (2022).
[32]P. Androvitsaneas *et al.*, "Direct-write projection lithography of quantum dot micropillar single photon sources," Appl. Phys. Lett. **123**(9), 094001 (2023).
[33]S. Liu *et al.*, "Dual-resonance enhanced quantum light-matter interactions in deterministically coupled quantum-dot-micropillars," Light Sci. Appl. **10**(1), 158 (2021).
[34]G. Mun, J. Gomis, B. Ale, L. Seravalli, P. Frigeri, and S. Franchi, "Exciton, biexciton and trion recombination dynamics in a single quantum dot under selective optical pumping," Physica E **40**, 2100–2103 (2008).
[35]Y. Benny, Y. Kodriano, E. Poem, and D. Gershoni, "Excitation spectroscopy of single quantum dots at tunable positive, neutral, and negative charge states," Phys. Rev. B **86**, 085306 (2012).
[36]S. Kreinberg *et al.*, "Quantum-optical spectroscopy of a two-level system using an electrically driven micropillar laser as a resonant excitation source," Light Sci. Appl. **7**(1), 41 (2018).
[37]P. Lodahl, S. Mahmoodian, and S. Stobbe, "Interfacing single photons and single quantum dots with photonic nanostructures," Rev. Mod. Phys. **87**(2), 347–400 (2015).
[38]M. Feucker, R. Seguin, S. Rodt, A. Hoffmann, and D. Bimberg, "Decay dynamics of neutral and charged excitonic complexes in single InAsGaAs quantum dots," Appl. Phys. Lett. **92**(6), 063116 (2008).
[39]A. V. Kuhlmann *et al.*, "Charge noise and spin noise in a semiconductor quantum device," Nat. Phys. **9**(9), 570–575 (2013).
[40]V. Scarani, H. Bechmann-Pasquinucci, N. J. Cerf, M. Dušek, N. Lütkenhaus, and M. Peev, "The security of practical quantum key distribution," Rev. Mod. Phys. **81**(3), 1301–1350 (2009).
[41]R. J. Young *et al.*, "Inversion of the exciton fine structure splitting in quantum dots," Physica E **32**(1–2), 97–100 (2006).
[42]T. M. Stace, G. J. Milburn, and C. H. W. Barnes, "Entangled two-photon source using biexciton emission of an asymmetric quantum dot in a cavity," Phys. Rev. B **67**(8), 085317 (2003).
[43]R. Seguin, A. Schliwa, S. Rodt, K. Potschke, U. W. Pohl, and D. Bimberg, "Size-dependent fine-structure splitting in self-organized InAs/GaAs quantum dots," Phys. Rev. Lett. **95**, 257402 (2005).
[44]R. Seguin *et al.*, "Control of fine-structure splitting and excitonic binding energies in selected individual InAs/GaAs quantum dots," Appl. Phys. Lett. **89**(26), 263109 (2006).
[45]R. M. Stevenson *et al.*, "Magnetic-field-induced reduction of the exciton polarization splitting in InAs quantum dots," Phys. Rev. B **73**(3), 033306 (2006).
[46]S. Seidl *et al.*, "Effect of uniaxial stress on excitons in a self-assembled quantum dot," Appl. Phys. Lett. **88**(20), 203113 (2006).